Soils and Foundations 2016;56(3):440–448

HOSTED BY

ELSEVIER

The Japanese Geotechnical Society

Soils and Foundations

www.sciencedirect.com
journal homepage: www.elsevier.com/locate/sandf

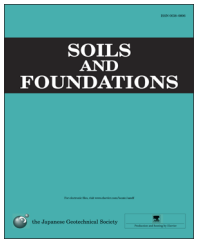

Technical Paper

PS wave based parallel seismic test for pile length assessment

Ye Du[a,b], Chunyu Song[a,*], Longzhu Chen[a], Jun Yang[a,c]

[a]*Institute of Engineering Safety and Disaster Prevention, Shanghai Jiao Tong University, Shanghai 200240, China*
[b]*College of Mining and Safety Engineering, Shandong University of Science & Technology, Qingdao, Shandong 266590, China*
[c]*Department of Civil Engineering, The University of Hong Kong, Hong Kong, China*

Received 6 February 2015; received in revised form 26 August 2015; accepted 3 March 2016
Available online 20 May 2016

Abstract

This paper presents an improved method for conducting parallel seismic tests to detect the unknown length and integrity of piles. The method involves the use of PS waves rather than the PP waves normally applied in conventional parallel seismic tests. Analytical solutions are derived for the *t–d* relationships of the first arrivals of the PS waves in homogeneous and layered soil conditions. Finite element models are also developed to simulate the waves generated by a vertical impact on the top of a pile under these two ground conditions for the purpose of validating the analytical solutions. The study indicates that the proposed method is viable and has several advantages over conventional parallel seismic tests.

Keywords: Parallel seismic test; Piles; Layered soil; Wave propagation; Non-destructive evaluation

1. Introduction

The parallel seismic (PS) test has been used for years to assess the integrity and the depth of existing piles (Olson et al., 1996; Kenai and Bahar, 2003; Herlein and Walton, 2007; Sack and Olson, 2009; Yu et al., 2010) and piles under construction (Wu and Yang, 2009; Huang and Ni, 2012). Compared to other non-destructive evaluation methods, this method is particularly useful in situations where the pile length is unknown or the pile head is not accessible for loading. As schematically shown in Fig. 1(a) and (b), the common practice of the method is to place a hydrophone in a borehole that has been drilled near the pile and filled with water. As the hydrophone is suspended in water, the signals received by the hydrophone are predominantly P waves, while S waves are filtered out. The P waves, traveling downward through the pile shaft and then transmitting to the soil, are referred to as PP waves, as shown in Fig. 2(a). Based on the time-versus-depth (*t–d*) relationship of the first arrivals of PP waves, the location of the pile base can be estimated as the point corresponding to the intersection depth of two fitting lines in the *t–d* plot, as shown in Fig. 2(b). This is the principle of conventional parallel seismic tests (Liao and Roesset, 1995; Liao et al., 2006; Huang and Chen, 2007; Lo et al., 2009; Ni et al., 2011; Huang and Ni, 2012; Niederleithinger, 2012; Lu et al., 2013; Zhang and Chen, 2013). Evidently, the slopes of the two fitting lines are affected by the velocity of the P waves in the pile and the velocity of the P waves in the soil below the pile tip.

For soil, its P-wave velocity (denoted as V_P^{soil}) is always higher than its S-wave velocity (denoted as V_S^{soil}), particularly in the case where the soil is saturated. The ratio of the two velocities can be determined as

$$\eta = V_P^{soil}/V_S^{soil} = \sqrt{2(1-\nu)/(1-2\nu)} \quad (1)$$

*Corresponding author.
E-mail address: chysong@sjtu.edu.cn (C. Song).
Peer review under responsibility of The Japanese Geotechnical Society.

http://dx.doi.org/10.1016/j.sandf.2016.04.010

where ν is Poisson's ratio of the soil and it increases with an increase in the degree of saturation of the soil (Du et al., 2013; Yang and Sato, 2000). For partially saturated soil, the value of ν typically ranges from 0.3 to 0.5, yielding $\eta > 1.87$, whereas for saturated soil, the value of ν approaches 0.5 leading to a sharp increase in η (Yang and Sato, 2000). In this context, for a pile installed in saturated soil, the difference between the P-wave velocity in the soil and that in the pile is much smaller than for a pile installed in unsaturated soil. Nevertheless, the difference between the S-wave velocity of the soil and the P-wave velocity of the pile remains almost unchanged in these two situations. Keeping this in mind, it is of great interest to investigate whether the S waves generated from the P waves transmitting from the pile to the surrounding soil can be used

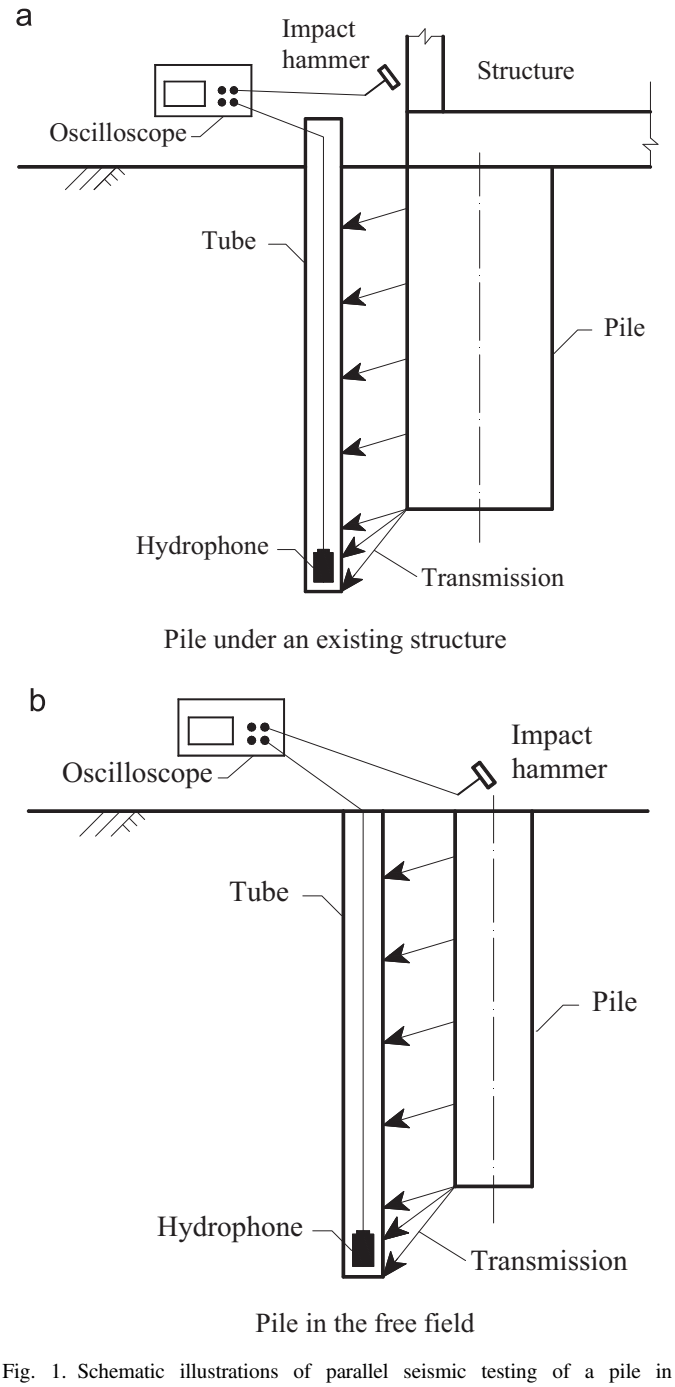

Fig. 1. Schematic illustrations of parallel seismic testing of a pile in homogeneous soil: (a) pile under an existing structure and (b) pile in the free field.

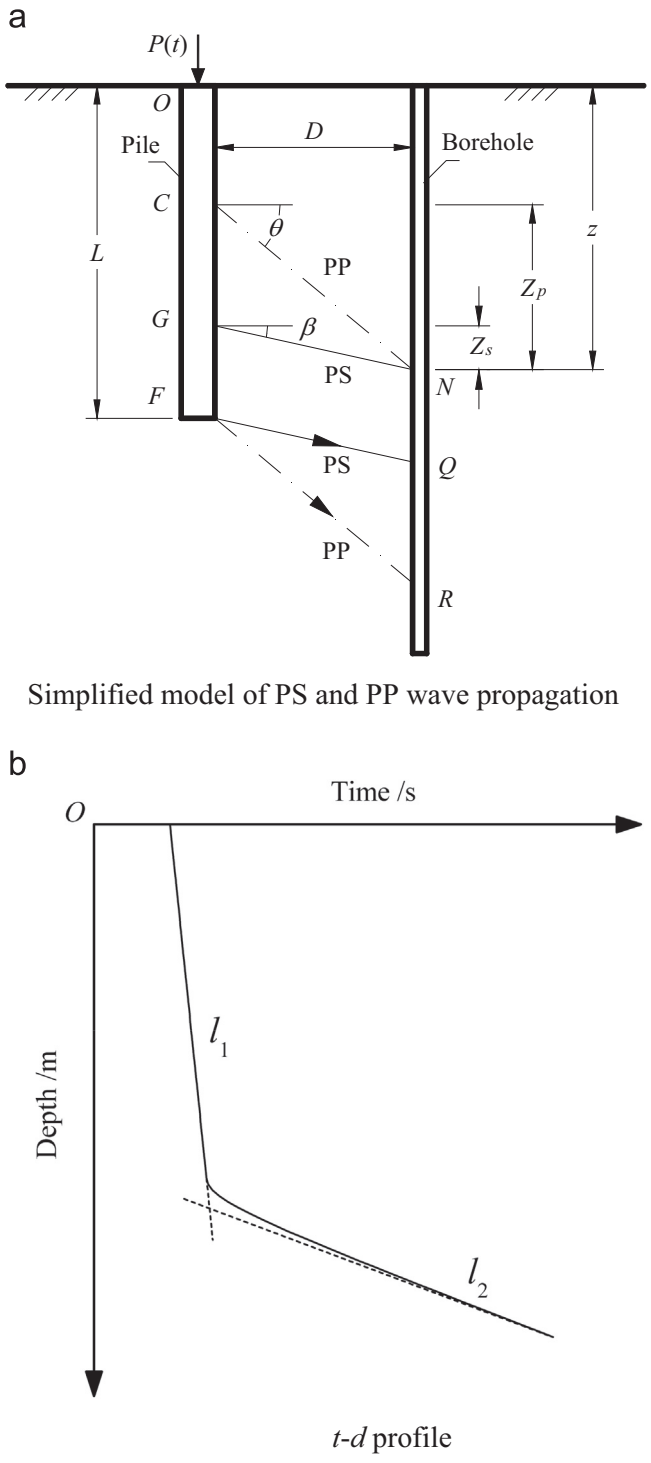

Fig. 2. Schematic illustrations of PS and PP wave-based tests for pile in homogeneous soil: (a) simplified model and (b) *t–d* profile.

to detect the pile length. The S waves are referred to as PS waves in this paper, as shown in Fig. 2(a).

In a parallel seismic test set-up, both PP and PS waves can be generated by an impact on the top of the pile or on the side face of the structure resting on the pile, and can be received at one time by a three-component geophone attached to the wall of the borehole at a given depth. An effort is made here to analyze the t–d relationship for the first arrivals of PS waves for simplified yet representative models so that an analytical method can be developed for practical applications.

2. Pile in homogeneous soil

Refer to Fig. 2(a) where a solid pile is installed in an elastic homogeneous soil. When a vertical impact load is applied on the pile top, PS waves are generated in the way shown in Fig. 2(a), where θ is the angle between the propagation path of a PP wave and the horizontal direction and β is the angle between the propagation path of a PS wave and the horizontal direction. According to the theory of wave propagation, the following relationships can be established:

$$\sin\ \theta = V_{\mathrm{P}}^{soil}/V_{\mathrm{P}}^{pile} = 1/n, \quad \sin\ \beta = V_{\mathrm{S}}^{soil}/V_{\mathrm{P}}^{pile} = 1/m \tag{2}$$

where V_{P}^{pile} is the velocity of the P wave in the pile. Obviously, because V_{S}^{soil} is less than V_{P}^{soil}, n is always less than m. Defining Z_p and Z_s as shown in Fig. 2(a), one has

$$Z_p = D\ \tan\ \theta = D/\sqrt{n^2-1}, \quad Z_s = D\ \tan\ \beta = D/\sqrt{m^2-1} \tag{3}$$

where D is the distance between the pile and the borehole.

Let z be the depth of the receiver which is located above point Q ($z = L+Z_s$), the first arrival time of the PS wave at this position is then determined as

$$t_s = \frac{z-Z_s}{V_{\mathrm{P}}^{pile}} + \frac{D}{V_{\mathrm{S}}^{soil}\ \cos\ \beta} \tag{4}$$

The substitution of Eqs. (2) and (3) into the above equation yields

$$t_s = \frac{1}{V_{\mathrm{P}}^{pile}} z + \frac{\sqrt{m^2-1}}{V_{\mathrm{P}}^{pile}} D \tag{5}$$

On the other hand, the first arrival time of the PS wave at an arbitrary position below point Q is

$$t_s = \frac{L}{V_{\mathrm{P}}^{pile}} + \frac{z-L}{V_{\mathrm{S}}^{soil}} \sqrt{1+\left(\frac{D}{z-L}\right)^2} \tag{6}$$

Note that if $z-L \geq 5D$, then $\sqrt{1+\left(\frac{D}{z-L}\right)^2} \approx 1$. Thus, Eq. (6) can be rewritten as

$$t_s = \frac{z}{V_{\mathrm{S}}^{soil}} - \frac{m-1}{m} \cdot \frac{L}{V_{\mathrm{S}}^{soil}} \tag{7}$$

In the above analysis, the three-dimensional wave propagation effect is ignored. The t_s–z relationship is a straight line with the slope of $1/V_{\mathrm{P}}^{pile}$ for $Z_s \leq z \leq L+Z_s$, as shown in Fig. 2(b) (line l_1), and for $z > L+5D$, it is approximately a straight line with the slope of $1/V_{\mathrm{S}}^{soil}$(line l_2). For $L+Z_s < z < L+5D$, it is a hyperbola and corresponds to the transition between the two straight lines.

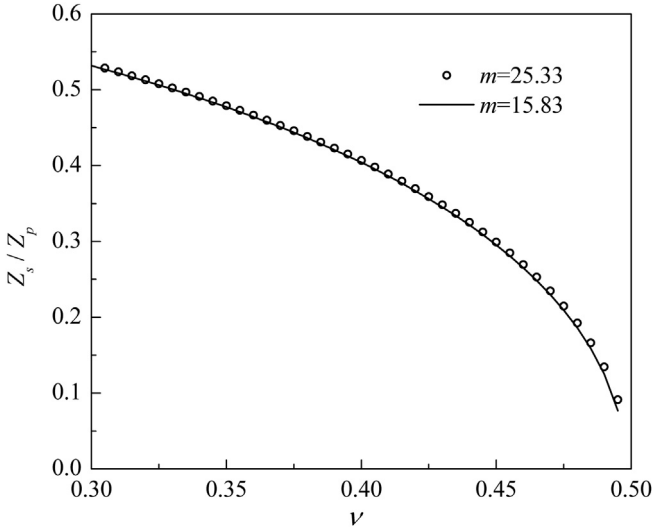

Fig. 3. Curves of Z_s/Z_p–ν.

According to Eqs. (1)–(3), the following relationship can be established:

$$\frac{Z_s}{Z_p} = \frac{1}{\eta}\sqrt{\frac{m^2-\eta^2}{m^2-1}} \tag{8}$$

Note that η is a function of Poisson's ratio of the soil. Fig. 3 shows the $Z_s/Z_p-\nu$ relation in which V_{P}^{pile} is taken as 3800 m/s and V_{S}^{soil} is assumed to be 150 m/s and 240 m/s, respectively. It is observed that the influence of the value of m on the $Z_s/Z_p-\nu$ relation is negligible. For a typical range of $0.3 < \nu < 0.5$, the value of Z_s/Z_p decreases sharply with an increase in ν, giving $0 < Z_s/Z_p < 0.54$. The value of Z_s/Z_p is 0.477 for a partially unsaturated soil with $\nu = 0.35$ and 0.091 for an almost saturated soil with $\nu = 0.495$. It is worth noting that the transmission depth of PS waves is much less than that of PP waves; for example, for $D = 1.5$ m, Z_s is 0.059 m and 0.095 m when V_{S}^{soil} is taken as 150 m/s and 240 m/s, respectively, both being smaller than 0.1 m. Hence, the traveling path of PS waves is inclined in the horizontal direction. When distance D is not large, the location of the pile base can be approximately treated as that corresponding to the depth of point Q (Fig. 2(a)) and it is not necessary to fit line l_2. This means there is no need to make the borehole longer than $(L+5D)$ (Du et al., 2012) and the cost of testing can be reduced.

3. Pile in layered soil

In reality, soil is not homogeneous, but rather inhomogeneous. A layered soil model is often used in practice to account for this in-homogeneity. Fig. 4 shows two representative models of layered soil: one is a weak layer i overlying a hard layer j and the other is a hard layer overlying a weak layer j. When the pile is subjected to a vertical impact load at its top, PS waves are generated at the boundary of the pile and the surrounding soil and they travel to a nearby borehole. Referring to Fig. 4(a), β_i is seen to be the angle between the propagation path of a PS wave

in soil layer i and the horizontal direction. The following relationships can be established:

$$\sin\beta_i = \frac{V_S^{soil\_i}}{V_P^{pile}} = \frac{1}{m_i}, \quad \cos\beta_i = \sqrt{m_i^2-1}/m_i,$$
$$Z_{si} = D\tan\beta_i = D/\sqrt{m_i^2-1} \tag{9}$$

where $V_S^{soil\_i}$ is the velocity of the S-wave in soil layer i. Generally, $m_i > 1$.

3.1 Soft layer overlying hard layer

Since the S-wave velocity of layer j is larger than that of layer i, $m_i > m_j$ is immediately obtained. For a PS wave traveling downward from layer i to layer j, the occurrence of complete reflection is possible. For this case, the critical angle of reflection (φ_i) can be determined as follows (Fig. 4(a)):

$$\sin\varphi_i = \frac{V_S^{soil\_i}}{V_S^{soil\_j}} = \frac{m_j}{m_i}, \quad \cos\varphi_i = \sqrt{m_i^2-m_j^2}/m_i,$$
$$\tan\varphi_i = m_j/\sqrt{m_i^2-m_j^2} \tag{10}$$

Note that H_i and H are the thickness of layer i and the surface layer above layer i, respectively.

Consider point N ($H < z < H+H_i$) along the borehole in layer i. Given the geometric relation shown in the figure

$$\overline{BE}+\overline{EN} = \frac{D}{\sin\varphi_i} = \frac{D}{m_j/m_i} \tag{11}$$

$$\overline{AN} = D/\cos\beta_i = D/\sqrt{1-(1/m_i)^2} \tag{12}$$

If $\overline{AN} > \overline{BE}+\overline{EN}$, then $1-(1/m_i)^2 < (m_j/m_i)^2$. That is, $m_i^2-m_j^2 < 1$. Note that the P-wave velocity in the pile is generally larger than the S-wave velocity in the soil. If the condition of $m_i^2-m_j^2 < 1$ is to be met, then the difference in the S-wave velocities in layer i and layer j must be extremely small. For example, given $V_P^{pile} = 3800$ m/s, $V_S^{soil\_i} = 149$ m/s and $V_S^{soil\_j} = 150$ m/s, it is found that $m_i^2-m_j^2 = 8.6 > 1$. However, the difference in the S-wave velocities of the two layers is only about 0.7%. For most situations, therefore, the conditions of $m_i^2-m_j^2 > 1$ and $\overline{AN} < \overline{BE}+\overline{EN}$ are satisfied, meaning that the travel time of the PS wave along the $A\to N$ path is less than that along the $A\to B\to E\to N$ path.

Let Δt_{N1} be the difference in travel times for the wave propagation along the $A\to B\to E\to F\to N$ path and along the $A\to B\to E\to N$ path. It can be determined as

$$\Delta t_{N1} = \frac{(H+H_i-z)\tan\varphi_i}{V_S^{soil\_j}} + \frac{H+H_i-z}{V_S^{soil\_i}} - \frac{H+H_i-z}{V_S^{soil\_i}\cos\varphi_i} \tag{13}$$

The above equation can be rearranged as

$$\Delta t_{N1} = \frac{H+H_i-z_i}{V_P^{pile}}\left(m_i - \sqrt{m_i^2-m_j^2}\right) > 0 \tag{14}$$

This shows that the travel time of the wave along the $A\to B\to E\to N$ path is less than that along the $A\to B\to E\to F\to N$ path.

Let Δt_{N2} be the difference in travel times of the wave propagation along the $A\to N$ path and along the $A\to C\to F\to N$ path. Then, the following is obtained:

$$\Delta t_{N2} = \frac{\overline{AN}}{V_S^{soil\_i}} - \left(\frac{\overline{AC}}{V_P^{pile}} + \frac{\overline{CF}}{V_S^{soil\_j}} + \frac{\overline{FN}}{V_S^{soil\_i}}\right) \tag{15}$$

where $\overline{AC} = H_i-(z-H)+Z_{si}$, $\overline{CF} = D$ and $\overline{NF} = H+H_i-z$. The substitution of these relations and Eq. (9) into Eq. (15) yields

$$\Delta t_{N2} = \frac{m_i+1}{V_P^{pile}}z + \frac{1}{V_P^{pile}}\left[D\sqrt{m_i^2-1}-(H+H_i)(m_i+1)-Dm_j\right] \tag{16}$$

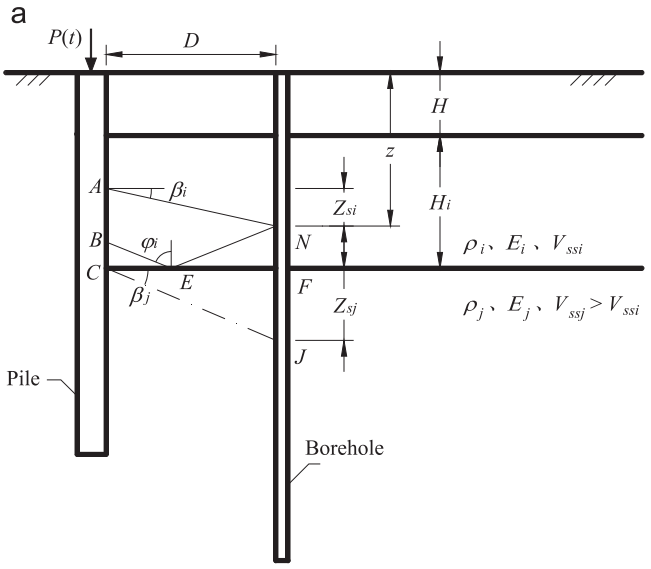

From soft layer to hard layer

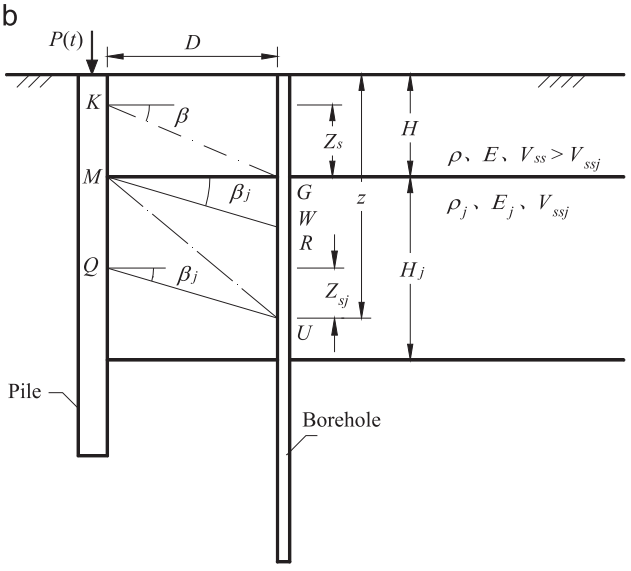

From hard layer to soft layer

Fig. 4. Schematic diagram of the simplified theoretical model of PST in layered soil: (a) from soft layer to hard layer and (b) from hard layer to soft layer.

Letting Eq. (16) be equal to zero, then

$$z_{sh1} = H + H_i + D\frac{m_j}{m_i+1} - D\sqrt{\frac{m_i-1}{m_i+1}} \tag{17}$$

Note that Δt_{N2} is an increasing function of z. Hence, if $z_{sh1} < H$, then $\Delta t_{N2} > 0$; if $z_{sh1} > H+H_i$, then $\Delta t_{N2} < 0$. For $H < z_{sh1} < H+H_i$, $\Delta t_{N2} > 0$ when $z > z_{sh1}$ and $\Delta t_{N2} < 0$ when $z < z_{sh1}$. The condition of $\Delta t_{N2} > 0$ means that the travel time of the PS wave along the $A \to C \to F \to N$ path is less than that along the $A \to N$ path, whereas the condition of $\Delta t_{N2} < 0$ means that the travel time of the PS wave along the $A \to N$ path is less. From the above analysis, there is no need to compare the propagation times of the PS waves traveling through the $A \to B \to E \to N$ path and the $A \to B \to E \to F \to N$ path with that traveling through the $A \to C \to F \to N$ path.

By calculating z_{sh1} from Eq. (17) and comparing it with z, the propagation time and the path of the first arriving PS wave can be determined for any position located between point N and point F in a borehole. When the receiver is located above point N and below point F in the layered soil, the travel time and the path of the PS wave are similar to those in a homogeneous soil.

3.2 Hard layer overlying soft layer

Referring to Fig. 4(b), it is assumed that the S-wave velocity of layer j is less than that of the surface layer. Obviously, $m_j > m > 1$. H_j and H denote the thicknesses of layer j and the surface above, respectively.

To investigate the propagation path of the first arriving PS wave at point U $(H+Z_{sj} < z < H+H_j)$ in layer j, the difference in travel times of the waves propagating through the $M \to Q \to U$ path and the $M \to U$ path is

$$\Delta t_{U1} = \left(\frac{z-H-Z_{sj}}{V_{\mathrm{P}}^{pile}} + \frac{D}{V_{\mathrm{S}}^{soil\_j}\cos\beta_j}\right) - \frac{\sqrt{D^2+(z-H)^2}}{V_{\mathrm{S}}^{soil\_j}} \tag{18}$$

Rearrangement of the above equation gives

$$\Delta t_{U1} = \frac{1}{V_{\mathrm{P}}^{pile}}\left[z - m_j\sqrt{D^2+(z-H)^2} - H + D\sqrt{m_j^2-1}\right] \tag{19}$$

Let $z-H=u$. If the right-hand side of Eq. (19) is greater than zero, then an inequality of $(u\sqrt{m_j^2-1}-D)^2 < 0$ is obtained. Obviously, this inequality does not hold; and hence, $\Delta t_{U1} < 0$. The travel time of the first arriving PS wave through the $M \to Q \to U$ path is less than that along the $M \to U$ path.

The difference in travel times of the waves propagating along the $K \to G \to U$ path and along the $K \to Q \to U$ path is

$$\Delta t_{U2} = \left(\frac{\overline{KG}}{V_{\mathrm{S}}^{soil}} + \frac{\overline{GU}}{V_{\mathrm{S}}^{soil\_j}}\right) - \left(\frac{\overline{KQ}}{V_{\mathrm{P}}^{pile}} + \frac{\overline{QU}}{V_{\mathrm{S}}^{soil\_j}}\right) \tag{20}$$

Given the geometries in Fig. 4(b), the following relations can be established:

$$\overline{GU} = z-H,\ \ \overline{KQ} = Z_s + z - H - Z_{sj},$$
$$\overline{KG} = D/\cos\beta,\ \ \overline{QU} = D/\cos\beta_j \tag{21}$$

Substitution of the above expressions and Eq. (9) into Eq. (20) yields

$$\Delta t_{U2} = \left(\frac{D}{V_{\mathrm{S}}^{soil}\cos\beta} + \frac{z-H}{V_{\mathrm{S}}^{soil\_j}}\right) - \left(\frac{Z_s+z-H-Z_{sj}}{V_{\mathrm{P}}^{pile}} + \frac{D}{V_{\mathrm{S}}^{soil\_j}\cos\beta_j}\right) \tag{22}$$

By rearrangement one has

$$\Delta t_{U2} = \frac{m_j-1}{V_{\mathrm{P}}^{pile}}z + \frac{1}{V_{\mathrm{P}}^{pile}}\left[D\sqrt{m^2-1} - D\sqrt{m_j^2-1} - (m_j-1)H\right] \tag{23}$$

Letting Eq. (23) be zero results in

$$z_{hs1} = H + \frac{D}{m_j-1}\left(\sqrt{m_j^2-1} - \sqrt{m^2-1}\right) \tag{24}$$

It is clear from Eq. (23) that Δt_{U2} is an increasing function of z. For $H+Z_{sj} < z < H+H_j$, $\Delta t_{U2} > 0$ when $z_{hs1} < H+Z_{sj}$, and $\Delta t_{U2} < 0$ when $z_{hs1} > H+H_j$. For $H+Z_{sj} < z_{hs1} < H+H_j$, $\Delta t_{U2} > 0$ when $z > z_{hs1}$ whereas $\Delta t_{U2} < 0$ when $z < z_{hs1}$. The propagation time along the $K \to Q \to U$ path is shorter compared with that along the $K \to G \to U$ path for $\Delta t_{U2} > 0$, but the propagation time along the $K \to G \to U$ path is smaller for $\Delta t_{U2} < 0$.

For the position W $(H < z < H+Z_{sj})$, located between point G $(z=H)$ and point R $(z=H+Z_{sj})$, the travel time difference for the wave along the $K \to G \to W$ path and the $K \to M \to W$ path is

$$\Delta t_W = \left(\frac{D}{V_{\mathrm{S}}^{soil}\cos\beta} + \frac{z-H}{V_{\mathrm{S}}^{soil\_j}}\right) - \left(\frac{Z_s}{V_{\mathrm{P}}^{pile}} + \frac{\sqrt{D^2+(z-H)^2}}{V_{\mathrm{S}}^{soil\_j}}\right)$$
$$= \frac{1}{V_{\mathrm{P}}^{pile}}\left[m_j\left(z - \sqrt{D^2+(z-H)^2} - H\right) + D\sqrt{m^2-1}\right] \tag{25}$$

Letting Eq. (25) be zero gives rise to

$$z_{hs2} = H + \frac{m_j^2 - m^2 + 1}{2m_j\sqrt{m^2-1}}D \tag{26}$$

Let $z-H=u$ in Eq. (25). Then, it is obvious that $u > 0$. Δt_W is an increasing function of u because

$$\frac{d(\Delta t_W)}{du} = \frac{m_j}{V_{\mathrm{P}}^{pile}}\left(1 - \frac{1}{\sqrt{1+(D/u)^2}}\right) > 0 \tag{27}$$

For the case of $H < z < H+Z_{sj}$, $\Delta t_W < 0$ if $z_{hs2} > H+Z_{sj}$. When z_{hs2} varies from H to $H+Z_{sj}$, $\Delta t_W > 0$ if $z > z_{hs2}$, and $\Delta t_W < 0$ if $z < z_{hs2}$. The wave propagation time along the $K \to M \to W$ path is less than that along the $K \to G \to W$ path for $\Delta t_W > 0$, whereas the propagation time along the $K \to G \to W$ path is less for $\Delta t_W < 0$.

The propagation time difference for the waves traveling through the $K \rightarrow G \rightarrow R$ path and the $K \rightarrow M \rightarrow R$ path is

$$\Delta t_R = \left(\frac{D}{V_S^{soil} \cos \beta} + \frac{Z_{sj}}{V_S^{soil\_j}}\right) - \left(\frac{Z_s}{V_P^{pile}} + \frac{D}{V_S^{soil\_j} \cos \beta_j}\right) = \frac{D}{V_P^{pile}}\left[\sqrt{m^2-1} - m_j\sqrt{\frac{m_j-1}{m_j+1}}\right] \quad (28)$$

It is noted that if

$$m > \sqrt{\frac{m_j^2(m_j-1)}{m_j+1}+1} \quad (29)$$

then the propagation path of the first arriving wave at point R is along the path $K \rightarrow M \rightarrow R$, otherwise it is along the $K \rightarrow G \rightarrow R$ path.

Comparing the value of z with that from Eqs. (24) and (26), and checking the value of m against the right-hand side of Eq. (29), the propagation path and the time of the first arriving PS waves can be obtained for the receiver located between point G and U in the borehole. For the receivers located in other positions, the propagation path and the time of the first arriving PS wave in the soft layer are the same as in a uniform soil.

In summary, the wave velocity in the soil surrounding the pile shaft, as well as the wave velocity in the soil beneath the pile base, must be taken into account in order to derive the propagation path and the time of the first arriving PS wave that travels downward from the pile to the soil.

4. Numerical model

In order to validate the analytical models derived above, an axisymmetric finite element model using ABAQUS is developed to simulate the wave propagation in a soil–pile system. Referring to Fig. 5, the pile in the model has a circular cross-section with a diameter of 0.6 m. Its length is 18 m and the distance from the pile to the borehole is 1.5 m. The soil profile is comprised of five layers with different P-wave and S-wave velocities. The physical and mechanical properties of the pile and the soils are given in Table 1. The force applied at the pile top is a half-cycle sine wave as given below.

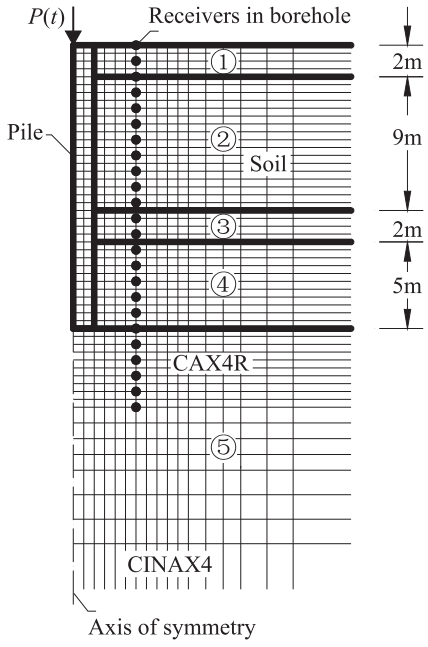

Fig. 5. Axisymmetric model for a pile in layered soil.

Table 1
Parameters of pile and soils.

	Density (kg/m^3)	Poisson's ratio	P-wave velocity (m/s)	S-wave velocity (m/s)	Thickness (m)
Pile	2400	0.2	3800	/	/
Soil 1	1700	0.4	500	205	2
Soil 2	1800	0.495	1500	150	9
Soil 3	1700	0.495	1200	120	2
Soil 4	1800	0.495	1500	150	5
Soil 5	1900	0.495	1700	170	/

$$P(t) = \begin{cases} P_0 \sin(\pi t/T_d), & 0 \le t \le T_d \\ 0, & t > T_d \end{cases} \quad (30)$$

where $P_0 = 1$ N , $T_d = 1.5$ ms.

Infinite element boundaries are used to account for the influence of artificially truncating boundaries. The model is divided into two regions, a finite element region and an infinite element region. CAX4R (four-node quadrilateral axisymmetric elements with reduced-integration) are used in the inner finite element region, and CINAX4 (four-node quadrilateral axisymmetric infinite elements) are used in the boundary region. Based on the velocities of the pile and the surrounding soil, and the spectral characteristics of the excitation at the pile top, the element size of the pile and the soil is taken as 5 cm and it increases with an increasing distance to the pile.

Fig. 6(a) and (b) shows the waveforms of the vertical and horizontal components of velocity at different depths. Comparing the waveforms of the vertical and horizontal components at the same depth, it is noted that the first arrivals and the predominant periods are different. The first arrival time and the predominant period of the waveform in the vertical component are apparently larger than those of the horizontal component. This difference is considered to be related to the characteristics of the excitation and the stiffness properties of the pile relative to the soil.

Under a vertical impact load on the pile top, the shear strain of the surrounding soil caused by the P waves traveling downward through the pile is larger than the normal strain in the radial direction resulting from the Poisson's effect of the pile shaft. When the P waves reach the pile base, the effect of the vertical dynamic stress on the soil beneath the pile is similar to that caused by a vertical dynamic load on the surface of a uniform soil.

Fig. 6 indicates that it is feasible to use PS waves in parallel seismic tests. Note in Fig. 6(a) that the first arrivals of the PS waves in depths between 1 and 2.5 m are significantly different from those of the PS waves below the depth of 2.5 m. This means that the soil below the depth of 2.5 m is softer than the

soil above this depth, which is consistent with the soil profile shown in Table 1. At depths of 11–13 m, there are significant changes in the first arrivals of the PS waves, indicating that the soil in this range of depth becomes softer. Fig. 6(a) also shows that PS waves at the depth of about 18 m appear to arrive earlier than those at lower depths and, in the meantime, the first arrivals of PP waves become clearer.

From the above interpretations, it is clear that the *t–d* relationship of the first arrivals of PS waves will change remarkably at depths where the properties of soils vary. To have a better view of the characteristics of waveforms received in the borehole near the pile and their relations to the pile length and integrity, the *t–d* relationships of the first arrivals of PS and PP waves are established from the numerical simulation, as shown in Fig. 7(a). It is noted that the *t–d* relationship of PS waves (FEM_PS) is more sensitive to changes in the soil profile in association with changes in the shear wave velocity. For the purpose of comparison, the analytical prediction of the *t–d* relationship for PS waves using the formulas derived in the preceding section is also shown in Fig. 7(a). A very good agreement is obtained between the numerical and the analytical results.

The *t–d* relationship, shown in Fig. 7(a), suggests that it is not appropriate to use a single straight line to represent the relationship for a pile in layered soil. For depths between 1–2 m, 2.5–11 m, 11.5–12.5 m and 13–17.75 m, the slopes of

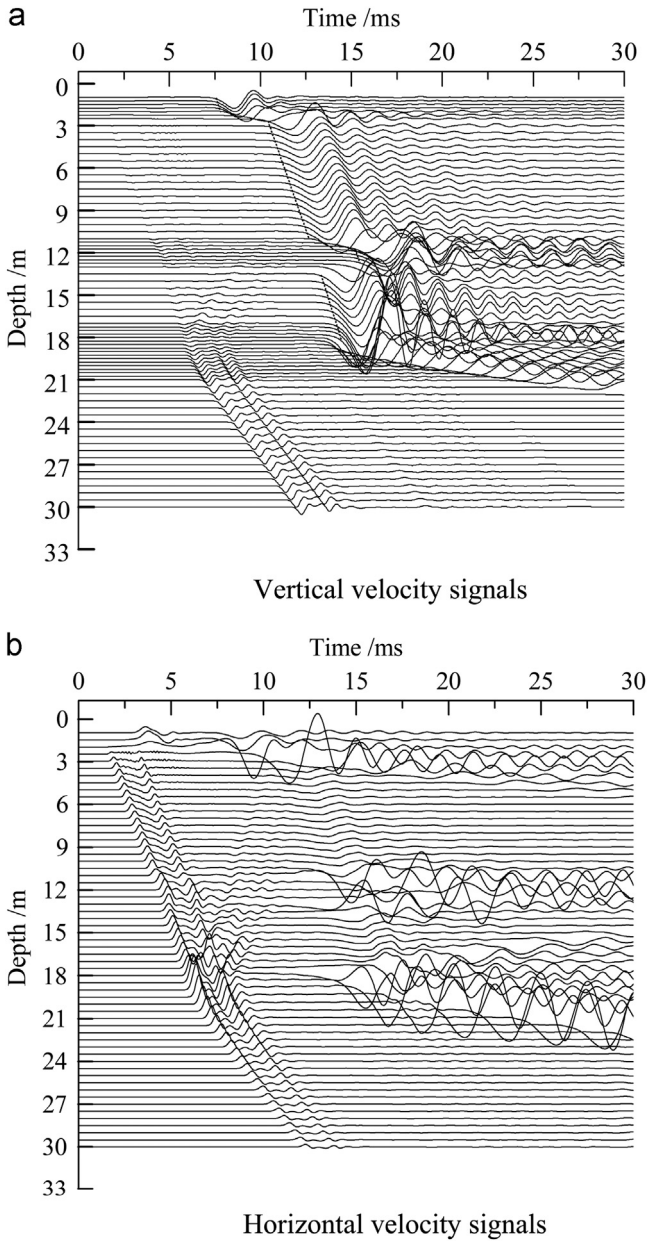

Fig. 6. Velocity signals in the borehole for foundation soil with a soft interlayer: (a) vertical velocity signals and (b) horizontal velocity signals.

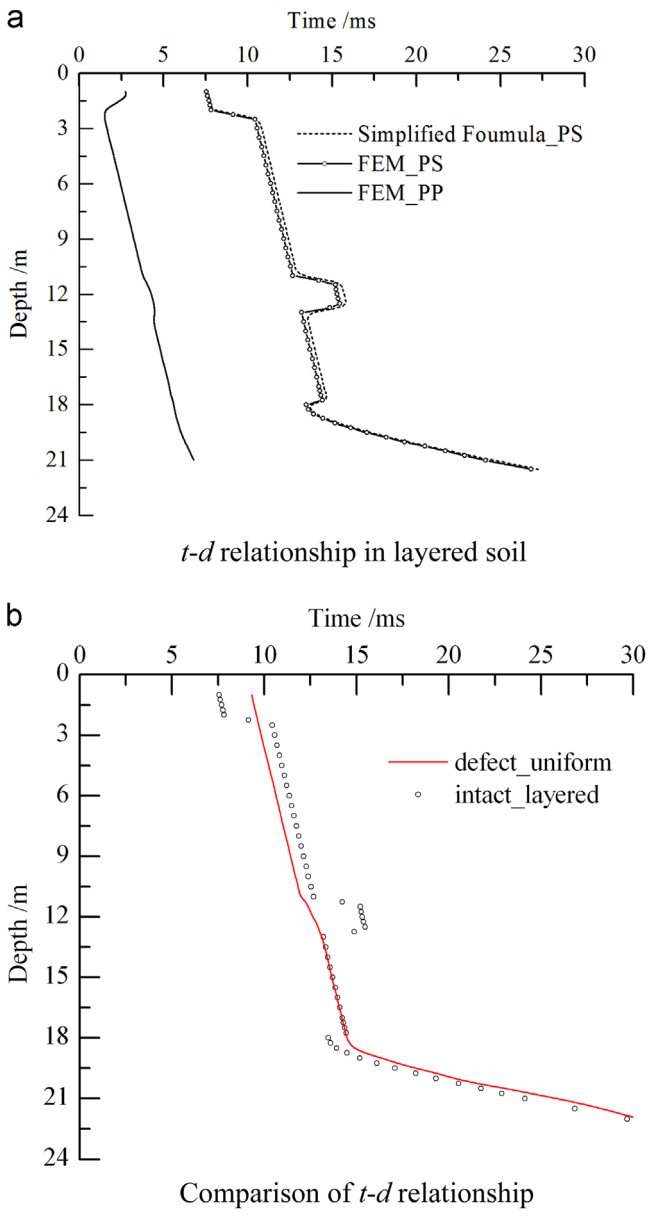

Fig. 7. Analysis of *t–d* relationship for the first arrival PS waves in layered soil: (a) intact pile in layered soil and (b) comparison with a defect pile in uniform soil.

fitting lines are determined to be 3710 m/s, 3813 m/s, 3878 m/s and 3858 m/s, respectively. These values are close to the P wave velocity in the pile. The transition zones between these four straight lines correspond to variations in the soil profile. At the depth around 18 m, there is a dramatic change in the slope of the fitted straight lines. As analyzed before, this depth corresponds to the location of the pile base.

To investigate the effect of pile defects on received waveforms, it is assumed that there is a defect between 11 and 13 m in the pile shaft, characterized by a low P-wave velocity (Du et al., 2013). The surrounding soil is assumed to be uniform and its properties are derived by averaging the soil properties in Table 1. The computed *t–d* relationship of the first arrivals of PS waves is shown in Fig. 7(b) along with that for the same pile without any defect in the layered soil. It is observed that the existence of a defect can also cause a change in the *t–d* relationship, but the change is not as significant as that caused by soil layering. Note that for both cases, the dramatic change in the slopes of fitted lines at the depth of about 18 m remains, suggesting that this characteristic is not affected by the integrity of the pile.

To further examine the applicability of the PS-wave based parallel seismic test to layered soil conditions where a hard soil layer exists, the original soil profile given in Table 1 is revised in the way that the properties of soft layer 3 are replaced by those of layer 5 with others unchanged. The numerical results for the *t–d* relationship of the PS wave are shown in Fig. 8 together with the analytical results obtained using the formulas derived before. Clearly there is a good agreement between numerical and analytical results. Both show that four straight lines can be identified in depths of 1–2 m, 2.5–10.75 m, 11.25–13 m and 13.5–17.75 m, giving the slopes of 3710 m/s, 3868 m/s, 3734 m/s and 3885 m/s, respectively. These values are close to the P-wave velocity in the pile (3800 m/s). The existence of the hard soil layer is reflected by a shift in the fitted line to the left at corresponding depths in the *t–d* plot. Again, the dramatic change in the *t–d* relationship at the depth of about 18 m is not affected by the existence of the hard layer in the soil profile.

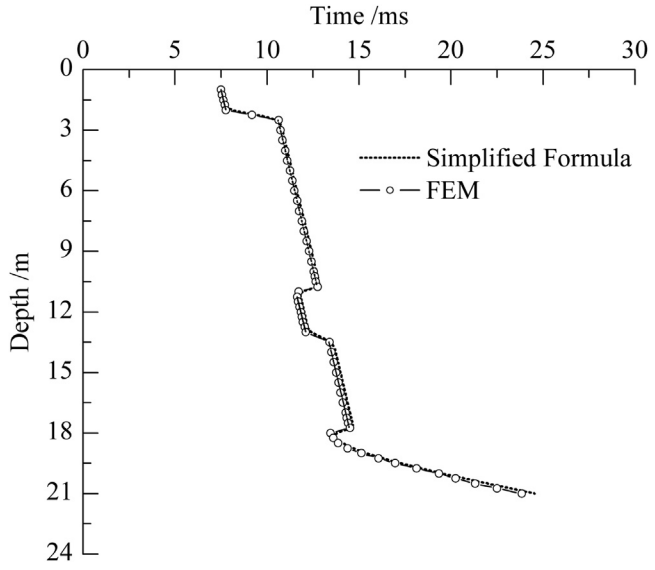

Fig. 8. Analytical and numerical *t–d* curves for the first arrival PS wave for the borehole in a layered ground with a hard interlayer.

5. Conclusions

This paper has presented a new idea for parallel seismic testing in which PS waves, rather than the conventional PP waves, are used to interpret the signals. Analytical solutions were derived for the *t–d* relationships of the first arrivals of received PS waves in both homogeneous soil and layered soil. Finite element models were also developed to simulate the waves generated by a vertical impact on the top of a pile in a homogeneous soil and in layered soil. The main results are summarized as follows:

(1) The first arrivals of PS waves are affected by soil layering as well as by the existence of defects in the pile shaft. This is manifested by changes in the *t–d* relationship along the pile shaft. It is recommended that a reliable soil profile (including P-wave and S-wave velocities) be established by means of field testing before conducting the parallel seismic test to detect the length and the integrity of the pile.
(2) The slope of the fitted straight line in the *t–d* plot for PS waves within the depths above the pile base corresponds to the one-dimensional P-wave velocity of the pile shaft. For a pile in layered soil, each soil layer is approximately represented by a fitted straight line in the *t–d* plot and between these lines are transition zones whose *t–d* relationship is not necessarily linear.
(3) In layered soil, the position of each fitted line in the *t–d* plot and the transitions between these lines are affected by the S-wave velocities of the soils surrounding the pile, the thickness of each soil layer, the P-wave velocity of the pile as well as the distance of the borehole to the pile.
(4) The change in the slope of the fitted line in the *t–d* plot caused by soil layering is visible only in depths corresponding to the soil layer, whereas the change in the slope of the fitted line caused by the existence of a defect is visible even below the defect depth.
(5) For both homogeneous and layered soil conditions, the position of the pile base can be clearly identified using the *t–d* relationship for the first arrivals of PS waves. The position corresponds to the depth where a dramatic change occurs in the slope of the *t–d* relationship. There seems no need to specify that the base of the borehole should be located below the pile base for a vertical distance of at least five times the distance between the pile and the borehole.

Acknowledgments

The work was supported by the National Nature Science Foundation of China (Nos. 51178267 and 51428901). This support is gratefully acknowledged. Jun Yang also wishes to express his thanks to Shanghai Jiao Tong University for the Distinguished Visiting Professorship.

References

Du, Y., Chen, L.Z., Ma, Y., 2012. Determination of pile length using parallel seismic testing with FEM simulation. J. Disaster Prev. Mitig. Eng. 32 (6), 731–736 (in Chinese).

Du, Y., Chen, L.Z., Zhang, J.Y., Yang, Y., Ma, Y., 2013. Analysis of defects of pile shaft for parallel seismic test. J. Shanghai Jiao Tong Univ. 7 (10), 1562–1579 (in Chinese).

Herlein, B.H., Walton, W.H., 2007. Project experience in assessment and reuse of old foundations. Contemporary Issues in Deep Foundations, 158. ASCE 1–10.

Huang, D.Z., Chen, L.Z., 2007. Studies on parallel seismic testing for integrity of cemented soil columns. Zhejiang Univ. Sci. A 8 (11), 1746–1753.

Huang, Y.H., Ni, S.H., 2012. Experimental study for the evaluation of stress wave approaches on a group pile foundation. NDT & E Int. 47, 134–143.

Kenai, S., Bahar, R., 2003. Evaluation and repair of Algiers new airport building. Cem. Concr. Compos. 25, 633–641.

Liao, S.T., Roesset, J.M., 1995. Determination of Pile Lengths using the Parallel Seismic Test. The University of Texas, Austin.

Liao, S.T., Tong, J.H., Chen, C.H., Wu, T.T., 2006. Numerical simulation and experimental study of parallel seismic test for piles. Int. J. Solids Struct. 43 (7–8), 2279–2298.

Lo, K.F., Ni, S.H., Huang, Y.H., Zhou, X.M., 2009. Measurement of unknown bridge foundation depth by parallel seismic method. Exp. Tech. 33 (1), 23–27.

Lu, Z.T., Wang, Z.L., Liu, D.J., 2013. A study on the application of the parallel seismic method in pile testing. Soil Dyn. Earthq. Eng. 55 (12), 255–262.

Ni, S.H., Huang, Y.H., Zhou, X.M., Lo, K.F., 2011. Inclination correction of the parallel seismic test for pile length detection. Comput. Geotech. 38 (2), 127–132.

Niederleithinger, E., 2012. Improvement and extension of the parallel seismic method for foundation depth measurement. Soils Found. 52 (6), 1093–1101.

Olson, L.D., Liu, M., Aouad, M.F., 1996. Borehole NDT techniques for unknown subsurface bridge foundation testing. SPIE 2946 (10), 10–16.

Sack, D.A. Olson, L.D., 2009. Combined parallel seismic and cone penetrometer testing of existing foundations for foundation length and evaluation. Geotechnical Special Publication 185, pp. 544–551.

Wu, B.J., Yang, H., 2009. Using parallel seismic and magnetic to detect length of prestressed concrete long tube pile. Qual. Test 27 (1), 27–29 (in Chinese).

Yang, J., Sato, T., 2000. Interpretation of seismic vertical amplification observed at an array site. Bull. Seismol. Soc. Am. 90 (2), 275–285.

Yu, X., Fang, J., Lin, G.M., 2010. Seismic CPTu to assist the design on existing foundations. Geotechnical Special Publication, 201. ASCE 169–177.

Zhang, J.Y., Chen, L.Z., 2013. Discussion of: a study on the application of the parallel seismic method in pile testing. Soil Dyn. Earthq. Eng. 55, 255–262.